Appendix

5.1 Coating photothermal effect in low-conductivity substrates

Assuming that the coating has the same thermal diffusivity as the substrate, we can calculate the coating's photothermal response by starting with the heat diffusion equation for half-space. The coating's thermal expansion is then determined by finding the average temperature of the mirror in a layer near the surface. I ignore the equation of elasticity, which is used on similar problems in [22, 23, 32], and which I expect to introduce corrections of order unity.

$$\begin{aligned} (\frac{\partial}{\partial t} - \frac{\kappa}{\rho C_v}\nabla^2)u(\vec{r},t) &= \frac{2P_0(f)\delta(z)e^{-(x^2+y^2)/r_0^2}}{\rho C_v \pi r_0^2} = F(\vec{r},t) \\ u(\vec{r},t)|_{z\to\infty} &= 0 \\ 0 \le z &\le \infty \end{aligned} \tag{5.1}$$

It is convenient to solve the Fourier transform of this equation. Letting $a^2 = \frac{\kappa}{\rho C_v}$,

$$u(\vec{r},\omega) = \frac{1}{2\pi^3}\int_{-\infty}^{\infty} d\vec{k}\frac{F(\vec{k},\omega)}{a^2k^2 + i\omega} \tag{5.2}$$

To select for temperature fluctuations near the surface, I follow the method of BGV [23] and use a weighting factor $e^{-z/l}/l$ to average over the zone near the surface. As measured by an interferometer, the response of the coating is given by the weighted average of $u(\vec{r},\omega)$ over a Gaussian beam spot with radius r_0. (The equations for integrating thermal expansion over the full thickness of the substrate are covered in [32].)

$$\bar{u}(\omega) = \frac{2P_0(\omega)}{\rho C(2\pi)^3}\int_{\vec{k},x,y=-\infty}^{\infty}\int_{z=0}^{\infty} d\vec{k}dxdydz\frac{e^{-z/l}}{l}\frac{e^{-(x^2+y^2)/r_0^2}}{\pi r_0^2}\frac{e^{-(k_x^2+k_y^2)r_0^2/4}}{a^2k^2+i\omega}e^{-i\vec{k}\cdot\vec{r}}$$

Evaluating the x, y, z integrals first gives

$$\bar{u}(\omega) = \frac{2P_0(\omega)}{\rho C(2\pi)^3}\int_{-\infty}^{\infty} d\vec{k}\frac{1}{1-ik_z l}\frac{e^{-(k_x^2+k_y^2)r_0^2/2}}{a^2k^2+i\omega} \tag{5.3}$$

Integrating next in k_z gives

$$\bar{u}(\omega) = \frac{P_0(\omega)}{\rho C(2\pi)^2}\int\int_{-\infty}^{\infty} dk_x dk_y \frac{e^{-(k_x^2+k_y^2)r_0^2/2}}{a\sqrt{a^2(k_x^2+k_y^2)+i\omega}-il(a^2(k_x^2+k_y^2)+i\omega)}$$

To evaluate this, take l to be the thermal diffusion length $r_t = \sqrt{\kappa/\rho C\omega} = a/\sqrt{\omega}$. This is difficult to compute at low frequencies, but at high frequencies, where $\omega \gg a^2/r_0^2$, we may ignore the terms in the denominator not proportional to $\sqrt{\omega}$. Noting that the dominant contribution to the integral comes when $k \approx 1/r_0$, we can approximate the displacement due to coating thermal expansion.

$$\begin{aligned}\bar{u}(\omega) &\approx \frac{P_0(\omega)}{\rho C(2\pi)^2}\int\int_{-\infty}^{\infty} dk_x dk_y \frac{e^{-(k_x^2+k_y^2)r_0^2/2}}{a\sqrt{a^2/r_0^2+i\omega}+a\sqrt{\omega}} \\ \bar{z}(\omega) &= \alpha d\bar{u}(\omega) \approx \frac{\alpha d P_0(\omega)}{\pi r_0^2\sqrt{\rho C_v\kappa\omega(1+i)}}\end{aligned} \tag{5.4}$$

Square this and replace $P(\omega)$ with the shot noise spectral density (see §2.4.1).

$$S_{\alpha,P}^{layer*}(f) \approx \frac{\alpha_{layer}^2 d^2 S_{abs}(f)}{4\pi^3 r_0^4\rho C_v\kappa f} \tag{5.5}$$

where d is the thickness and α is the thermal expansion coefficient of the coating.

5.2 Cross-coupling noise

To derive equations 3.9 and 3.10, I assume weak modulation depth at the EOM, so that only the carrier and first-order sidebands of the *probe* beams are significant. Following the formalism of Day [41], the light falling on the cavity on resonance is

$$\begin{aligned} P_0 &= |E_r + E_u|^2 \\ E_r &= \sqrt{P_C}e^{i\varpi t} + i\sqrt{P_S}\sin(\Omega t)e^{i\varpi t} \quad (5.6) \\ E_u &= \sqrt{P_F}e^{i\varpi t}e^{i\phi} \quad (5.7) \end{aligned}$$

where ϖ is the light frequency, Ω is the sideband modulation frequency, and ϕ is a random phase shift, not necessarily stationary in time.

The *probe* beam field can be expanded as

$$E_r = \sqrt{P_C}e^{i\varpi t} + i\sqrt{P_S/2}(e^{i(\varpi+\Omega)t - e^{i(\varpi-\Omega)t} \quad (5.8)$$

The amplitude reflection coefficient depends on the input (r_1) and test (r_2) mirror amplitude reflectivities and input mirror losses (L_1). Lower-case letters indicate field coefficients, while capital letters apply to power.

$$A(\varpi) = \frac{r_2(1-L_1)e^{i\varpi/FSR} - r_1}{1 - r_1 r_2 e^{i\varpi/FSR}} \quad (5.9)$$

The quantity ϖ/FSR may be replaced by $4\pi\Delta L/\lambda$ to convert frequency shifts to length changes. The field reflected from the cavity is

$$\begin{aligned} E_{refl} &= |\sqrt{P_F}e^{i\varpi t}e^{i\phi}A(\varpi) + \sqrt{P_C}e^{i\varpi t}A(\varpi) + \\ &\quad \sqrt{P_S}e^{i(\varpi+\Omega)t}A(\varpi+\Omega) - \sqrt{P_S}e^{i(\varpi-\Omega)t}A(\varpi-\Omega) \quad (5.10) \end{aligned}$$

The polarizing optics split the *pump* and *probe* beams on their return paths, and direct the *probe*

beam, and a small amount of the *pump* beam, toward the RFPD. Between the IFO and the photodiode, the light power is attenuated overall by various filters and transmissive optics, so that the field that we measure at the RFPD is proportional to

$$\begin{aligned} E_{PD} \quad \propto \quad & \zeta\sqrt{P_F}e^{i\varpi t}e^{i\phi}A(\varpi) + \sqrt{P_C}e^{i\varpi t}A(\varpi) + \\ & \sqrt{P_S}\left[e^{i(\varpi+\Omega)t}A(\varpi+\Omega) - e^{i(\varpi-\Omega)t}A(\varpi-\Omega)\right] \end{aligned} \tag{5.11}$$

If the demodulation phase at the mixer is chosen to maximize the zero-crossing slope of the PDH signal, then the maximum amount of systematic error due to polarization crosstalk will occur when $\phi \to 0$ or π. Consider all four fields as phasors. The sum of the carrier and force fields is a field in phase with the carrier. The PDH signal arises from the beat between the carrier (or the sum of the carrier and the noise field) and the two sidebands.

The optical power reaching the photodiode is $P_{PD} = |E_{PD}|^2$. After some algebra, this may be written as

$$\begin{aligned} P_{PD} \quad \propto \quad & \zeta^2 P_F + P_C + 2\zeta\sqrt{P_C P_F}\cos(\phi)|A(\varpi)|^2 + \\ & 2\sqrt{P_S P_C}\{\Re\left[A(\varpi)A^*(\varpi+\Omega) - A^*(\varpi)A(\varpi-\Omega)\right]\cos\Omega t + \\ & \Im\left[A(\varpi)A^*(\varpi+\Omega) - A^*(\varpi)A(\varpi-\Omega)\right]\sin\Omega t\} + \\ & 2\sqrt{P_S P_C}\{\Re\left[A(\varpi)A^*(\varpi+\Omega)e^{i\phi} - A^*(\varpi)A(\varpi-\Omega)e^{-i\phi}\right]\cos\Omega t + \\ & \Im\left[A(\varpi)A^*(\varpi+\Omega)e^{i\phi} - A^*(\varpi)A(\varpi-\Omega)e^{-i\phi}\right]\sin\Omega t\} \\ & +2\Omega\ terms... \end{aligned} \tag{5.12}$$

The terms proportional to $\sqrt{P_F P_S}$ may be simplified. In the linear region of the PDH signal, near a cavity resonance,

$$F(\varpi)F^*(\varpi+\Omega) \quad = \quad -F(\varpi)F^*(\varpi-\Omega) \tag{5.13}$$

Using this approximation, we arrive at

$$
\begin{aligned}
P_{PD} \quad \propto \quad & \zeta^2 P_F + P_C + 2\zeta\sqrt{P_C P_F}\cos(\phi)|A(\varpi)|^2 + \\
& 2\sqrt{P_S}(\sqrt{P_C} + \zeta\sqrt{P_F}\cos(\phi))\{\Re\left[A(\varpi)A^*(\varpi+\Omega) - A^*(\varpi)A(\varpi-\Omega)\right]\cos\Omega t + \\
& \Im\left[A(\varpi)A^*(\varpi+\Omega) - A^*(\varpi)A(\varpi-\Omega)\right]\sin\Omega t\} \\
& +2\Omega\ terms... \qquad (5.14)
\end{aligned}
$$

The photodiode measures high frequency (P_{RF}) and low frequency (P_{DC}) components of the optical field separately. Because the mirror reflectivities are not perfectly matched in this experiment, the P_{DC} is non-zero at resonance.

$$
\begin{aligned}
P_{DC} &= |A(0)|^2\left(P_C + 2\zeta\sqrt{P_F P_C}\cos\phi + \zeta^2 P_F\right) \qquad (5.15) \\
A(0) &= \frac{r_2 - r_1}{1 - r_1 r_2} \qquad (5.16)
\end{aligned}
$$

The PDH signal consists of the components of P_{RF} at the sideband frequency, Ω. The low frequency component of this is converted into the measured PDH signal.

$$
\begin{aligned}
V_{PDH} \quad = \quad & V_0\{\Re\left[A(\varpi)A^*(\varpi+\Omega) - A^*(\varpi)A(\varpi-\Omega)\right]\cos\theta + \\
& \Im\left[A(\varpi)A^*(\varpi+\Omega) - A^*(\varpi)A(\varpi-\Omega)\right]\cos\theta\} \qquad (5.17)
\end{aligned}
$$

where θ is the phase shift between the local oscillator and RF inputs at the mixer and V_0 is an arbitrary scale factor.

Cross-coupling can be measured directly with the instrument's polarizing optics set poorly and the cavity off resonance. Measurements of the variations in the PDH signal under these conditions show that the cross-coupling noise is proportional to the square roots of both the carrier and sideband power. Fig. 5.1 plots the cross-coupling for a variety of *pump* and *probe* powers.

Figure 5.1: Cross-coupling dependence on beam power. Left: *probe* power = 16 mW. Right: *probe* power = 26 mW. Data are fit to $P_F^{1/2}$.

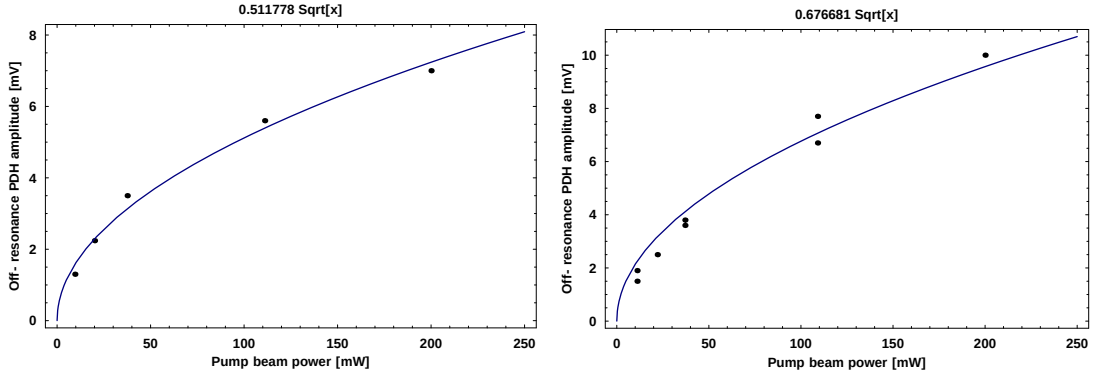

5.3 Interferometer identities

In a Fabry-Perot interferometer, the Finesse is the ratio of the line width (FWHM of transmitted power) to the free spectral range (FSR). In frequency units, the FSR is $c/2L$. In length units, it is $\lambda/2$. The conversion factor from frequency to length is simply $\lambda L/c$. The various reflection and transmission coefficients for lossy, asymmetric cavities on resonance are

$$\begin{aligned} Reflection &= \left(\sqrt{R_1} - T_1 \sum_0^\infty (R_1R_2)^{n/2}\right)^2 \\ &= \left(\sqrt{R_1} - \frac{\sqrt{R_2}T_1}{1-\sqrt{R_1R_2}}\right)^2 \qquad (5.18) \\ Transmission &= T_1T_2\left(\sum_0^\infty (R_1R_2)^{n/2}\right)^2 \\ &= \frac{T_2T_1}{(1-\sqrt{R_1R_2})^2} \qquad (5.19) \\ Buildup &= T_1\left(\sum_0^\infty (R_1R_2)^{n/2}\right)^2 \\ &= \frac{T_1}{(1-\sqrt{R_1R_2})^2} \qquad (5.20) \end{aligned}$$

Note that $T_1 + R_1 \leq 1$ and $T_2 + R_2 \leq 1$.

5.4 TNI

5.4.1 Mode cleaner electronics

The K_{boost} amplifier in the mode cleaner servo (see §4.7) is critical for lock acquisition. It has two $\times 10$ boost stages at low frequency to increase the DC gain of the servo without affecting its unity gain point. Fig. 5.3 It can be used as a low-noise variable-gain inverting amplifier, with a single boost enabled, or with both boosts enabled[1]. It is mounted in a single-width NIM box and requires ± 24 V, regulated down to ± 15 V. The circuit is built in three stages, each based on the AD797 high-speed op amp. The first stage (*gain*) is a variable-gain amplifier with two inputs. In_1 has an input impedance of 1 kΩ and a range of ± 15 V. In_2 is limited to 800 mV_{pp} and, for small signals, has a 4.7kΩ input impedance. The response of the first stage is $V_1 = -G(In_1 + In_2/4.7)$. The second and third stages (*boost2, boost2*) are switchable lags: With the switch closed, they are unity-gain inverting amplifiers. With the switch open, their response is $V_2 = -100(V_1(if + 10000)/(if + 100))$. The front panel has BNC connectors for the inputs and outputs, a knob to adjust the gain (VR1), and switches (SW1, SW2) to enable the boosts. The recommended operating range for the gain knob is from 0.4 to 9.5.

The amplifier's input referred noise is 5 nV/rHz at each op-amp stage. There appears to be some high-frequency resonance, possibly because of the inductance of the twisted-pair wires connecting the circuit board to SW1 and SW2 on the front panel. The amplifier also picks up an oscillation at 80 MHz, possibly from an FM broadcast. There is an input offset at each stage of about 100 mV, depending on temperature. Input offsets are adjustable for each chip with trimpots on the circuit board.

[1] See the *North Arm Cavity and Beyond* lab notebook, page 114.

Figure 5.2: Schematic of reflection and transmission used in deriving the above formulae. $\sqrt{R_1} = r_1$, etc.

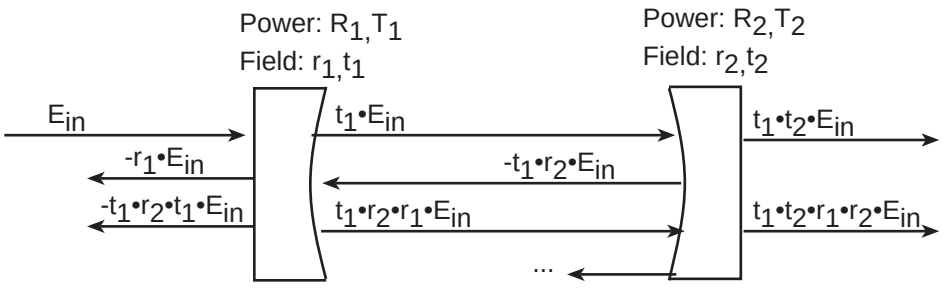

Figure 5.3: Boost amplifier circuit schematic

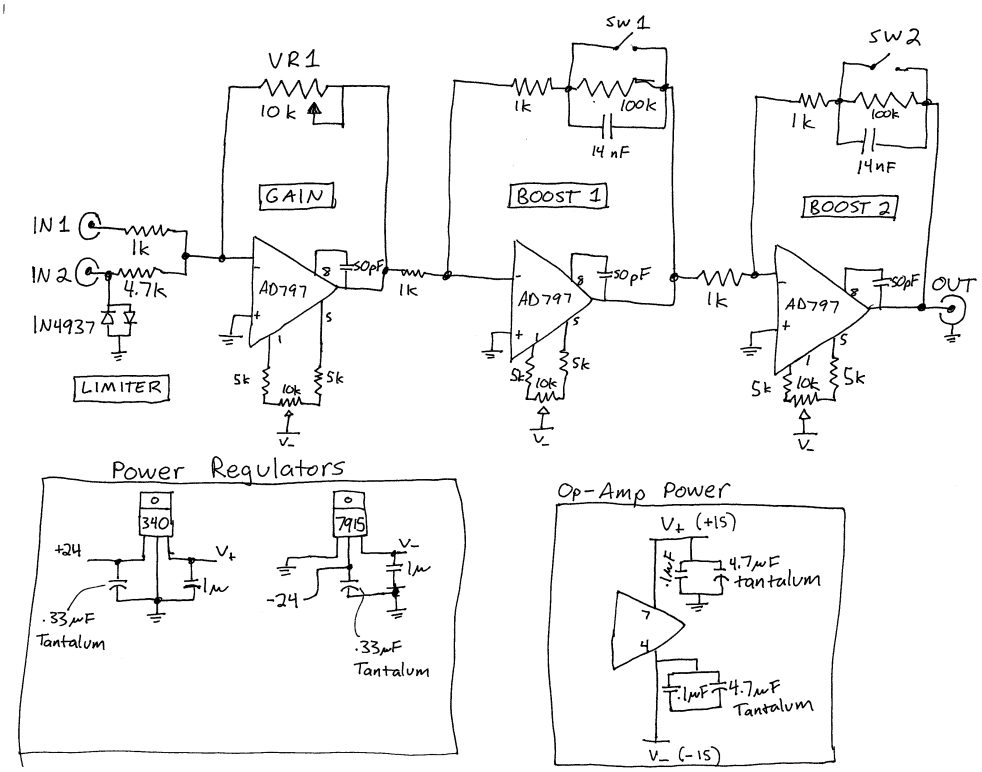

As an inverting amplifier with both boosts off, phase lag is less than 5° at 100 kHz. Either of the two identical boost stages may be activated with the front-panel switches. A transfer function of the amplifier with one boost shows a pole at 100 Hz, a zero at 10 kHz, and a DC gain of 40 dB. Phase lag for each boost at 100 kHz is less than 6°. Fig. 5.4 shows the measured transfer functions for the inverting amplifier configuration and for one boost enabled.

5.4.2 Alignment procedure

The first step to aligning the TNI is to balance the instrument table in the vacuum chamber. If the table is not level, it can drift and tilt enough over a few days to displace the suspended mirrors by more than a millimeter. So all the optics need to be assembled and the table balanced before you can align the beam to the cavities.

It can be difficult to find the resonant axis of the mode cleaner. You should set up a HeNe laser on the auxiliary table, and send it backwards through the mode cleaner. Since dielectric mirrors designed for 1 micron partially reflect red light, the mode cleaner will form a low finesse ring cavity for the HeNe beam. When the HeNe is aligned to the mode cleaner, there is a transmitted bull's-eye

Figure 5.4: Left: inverting amplifier (no boosts). Right: one boost active.

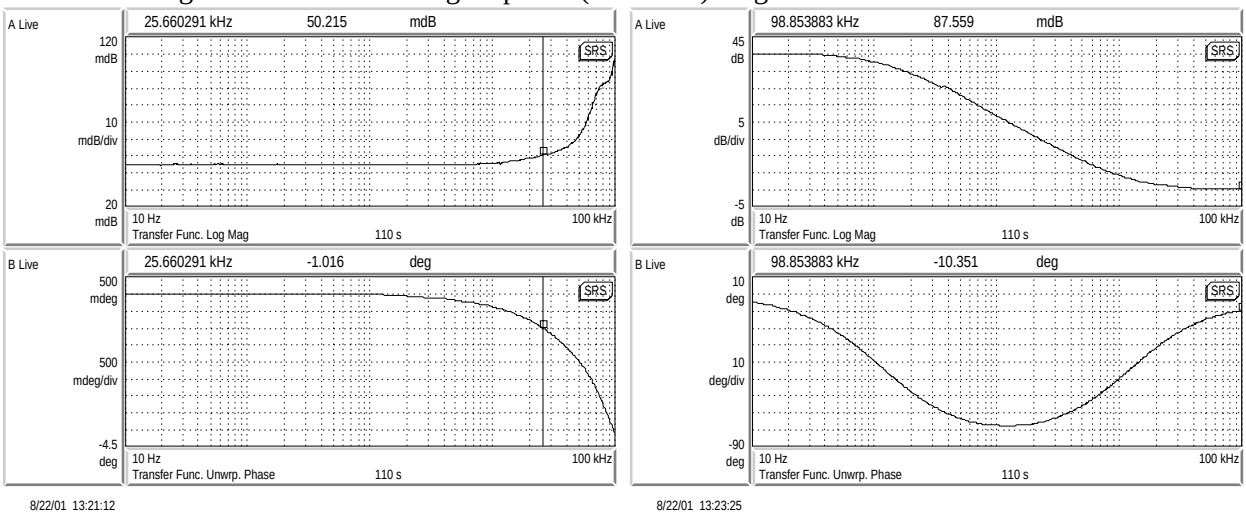

pattern that shifts as the mirrors swing in response to air currents. The cavity is properly aligned the laser when this beam overlaps the NPRO beam.

5.5 Calibration procedure

There are two ways to calibrate the interferometer responses. The simplest is to let the mirror swing through a resonance while measuring the slope of the PDH signal. The other is to measure the open-loop transfer function of the servo, and divide it by the gains of all the components except for the interferometer response. These procedures can be accurate to within 10-20%. A better calibration method would use a photon drive.

5.5.1 OSEM optimization procedure

Local damping works best when the center of the OSEMs' dynamic range coincides with the natural resting position of the mirror. On the mode cleaner, the OSEM circuit boards are constructed such that the LED will burn out if the board contacts touch any piece of grounded metal, such as the insulation on the cables.

1. Turn off the controller.

2. Remove all the sensor/actuators from the suspension. Place them on the table in such a way that you will remember where they belong. Be careful that the circuit boards aren't touching anything metallic. If they do, the LED will blow out and need to be replaced.

3. Set the yaw, pitch, and Z switches to *global* mode to disable feedback.

4. Turn the controller on. Turn all the offset pots to 5.00. The gain knobs have no effect.

5. Insert an OSEM into the suspension. Start with the one that is in the most awkward position (usually LL or LR). Connect the Local Position Monitor signal for this sensor to both input channels of an oscilloscope. Set one of the scope channels to 5 V/div and the other to 0.1 V/div.

6. Move the sensor/actuator around in the SOS until its position measures zero. Tighten the set screw to hold it in place.

7. Repeat steps 5-6 for the remaining mirror-back OSEMs, but not for the horizontal one yet.

8. Re-check all the local position signals. Inspect the front of the mirror and make sure that no fins rub against the inside of the OSEMs.

9. Set the yaw, pitch, and Z switches to *local* mode. The mirror should damp in these degrees of freedom, but is still free to swing from side to side.

10. Insert the horizontal sensor/actuator, monitoring its position as in step 5.

11. Increase the side channel gain on the OSEM controller.

12. The mirror should damp in all degrees of freedom.

5.5.2 Venting the vacuum chamber

1. Check all vacuum gauges. The cold cathode gauge should reach 10^{-6} Torr.

2. If the turbo pump is on, it should say “Normal Operation 56 krpm.”

3. Close all valves to the vacuum chamber. Flip the switch on the gate valve controller box to “close”. Turn the handle on the roughing valve to close it. Turn the handle on the vent valve clockwise to close it.

4. To turn the turbo pump off, press the “Start/Stop reset” button on the controller. The turbo pump controller will say “Ready for local soft start.” The turbo pump and the fan will both stop. After five seconds, the vent valve for the turbo pump will open. Air coming into the

pump will slow down the pump, and you will be able to hear the whine as it spins down. Turn the turbo pump controller off, then turn the diaphragm pump off.

5. Turn the cold cathode gauge off.
6. The roughing valve should be closed, so that the catalyzer trap stays hot and under vacuum.
7. Vent the chamber by slowly opening the vent valve (counterclockwise). Air will flow in for about 20 minutes.